The Nucleus **50**, No. 4 (2013) 395-409

The Nucleus
A Quarterly Scientific Journal of Pakistan Atomic Energy Commission
NCLEAM, ISSN 0029-5698

SUPER-TWISTING SLIDING MODE CONTROL STRATEGY FOR DYNAMIC VOLTAGE RESTORER TO IMPROVE POWER QUALITY IN POWER DISTRIBUTION SYSTEM

*S. KANWAL and A. HANIF

Department of Electrical Engineering, Wah Engineering College, University of Wah, Wah Cantt, Pakistan

(Received September 10, 2013 and accepted in revised form November 29, 2013)

The paper deals with application of super-twisting sliding mode control in Dynamic Voltage Restorer (DVR) to tackle various Power Quality (PQ) issues. The various features of super-twisting sliding mode, which include selection of sliding surface, stability of system, existence of sliding mode and reaching conditions to bring system states on sliding surface, are discussed for mitigation of voltage sag/swell and phase jumps applications. Pulse width modulation (PWM) based second order super-twisting sliding mode control is used to operate voltage source converter (VSC) in voltage control mode for mitigation of voltage sag, voltage swell and phase jumps to regulate power flow to load. The proposed controller design is simulated for single phase DVR. It exhibits robustness to system parameters and load variations. The load voltage Total Harmonic Distortion (THD) is calculated to evaluate the voltage quality. MATLAB®/Simulink® SimPowerSystem tool box is used to check the performance of proposed control strategy. Simulation results show that response time and chattering effect can be minimized with use of super-twisting sliding mode control while keeping the main properties of standard sliding mode control (SMC). The proposed control scheme can compensate voltage sags, voltage swells and phase jumps within 2ms which is reasonably lower than ITIC curve and SEMI-F-47 standard for sensitive loads that suggest a tolerable time limit of 20ms.

Keywords : Dynamic voltage restorer, Voltage sag, Voltage swell, Sliding mode, Sliding manifold, Super-twisting sliding mode

1. Introduction

Non-linear and sensitive loads have created tremendous impact on Power Quality (PQ) in distribution network. Major financial losses in industries are accompanied with voltage sags, voltage swells, and phase jumps [1]. Power electronics equipment, adjustable speed drives, PLCs, motor contactors and other nonlinear loads are increasing concerns of power quality [2]. Electrical utilities are trying to deal with these problems to supply high quality nearly smooth sinusoidal power with desired magnitude. Voltage sag is stated as the reduction in voltage amplitude (10% - 90% of nominal voltage) for half cycle to 1 min according to IEEE Standard 1159-1995, while voltage swell is increase of voltage amplitude (110% - 180% of nominal voltage) for half cycle to 1 min. [3]. Thus these PQ problems are defined for specific magnitude and duration in available utility voltage [4]. ITI and SEM have provided curves showing equipment ride-through capability for voltage sag of different magnitude and durations [5]. An effective solution of PQ problems in power distribution network is installation of Custom Power Devices (CPDs). Voltage sag, voltage swell and phase jumps are effectively handled using series CPDs like Dynamic Voltage Restorer (DVR) [6-7]. To regulate power delivery to load, compensated voltage is injected by DVR through injection transformer. The DVR main purpose is to detect any disturbance and mitigate that disturbance to regulate voltage in distribution system [8-9]. Control strategies which may be linear or non-linear can be employed for the generation of control signals to voltage source converter (VSC)[10]. The generation of these control signals determines the DVR performance efficiency [11]. Output of VSC is filtered by LC filter and injected at PCC. The block diagram of distribution system with DVR connected in series is given in Figure 1 [12].

Conventional control methods of CPDs employing classical/modern control algorithms are sensitive to external parameter variations [13]. Thus an efficient control technique is required which can operate in all conditions with high stability [14]. A nonlinear close loop control strategy with fuzzy interference into sliding mode control is proposed [15]. In ref. [16] a nonlinear method based controller of DVR protects sensitive loads from adverse effects of voltage sag. For mitigation of voltage sag and voltage swell

* Corresponding author : skanwal_26@yahoo.com

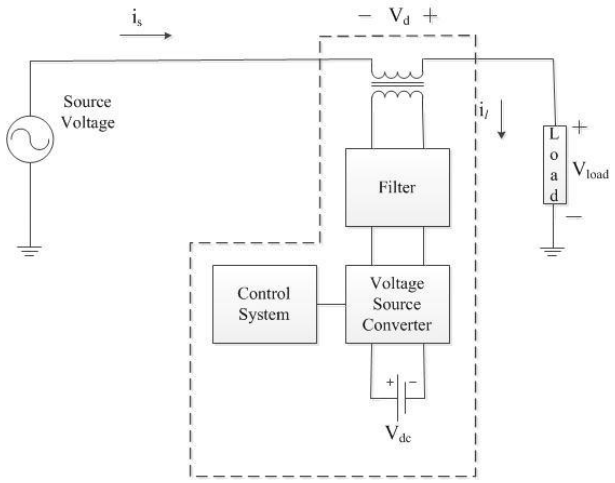

Figure 1. Single phase conventional DVR based distribution system [12].

symmetrical component based control strategy was suggested in [17]. In [18], a hybrid feed forward and feedback control strategy was introduced. The strategy proposed in [19] mitigates voltage sag by optimal amount of energy injection with phase advance compensation scheme. The proposed control technique is based on closed loop super-twisting sliding mode which is very effective and robust technique to external disturbance [20]. The sliding mode brings states of system to a surface which can change the structure of close loop control thus to gain certain output [21]. The formulated equations through derived mathematical model of super-twisting sliding mode control provides guidelines to restore load voltage to its nominal value. The proposed controller is validated using MATLAB®/ SIMULINK® SimPowerSystems™ Simulations, for a test system.

2. Mathematical Model

Two steps are required for implementation of sliding mode control (SMC): The first one is selection of a sliding surface. When the state trajectory is constrained on the selected sliding line, the DVR exhibits the desired performance. The next step forces the system state to reach and stay on that sliding manifold in finite time. The derived state space model is based on DVR circuit shown in Figure 2.

Load voltage V_{load} is equivalent to sum of voltage V_D injected by DVR alongwith source voltage V_{source} as given in equation (1).

$$V_{load} = V_{source} + V_D \tag{1}$$

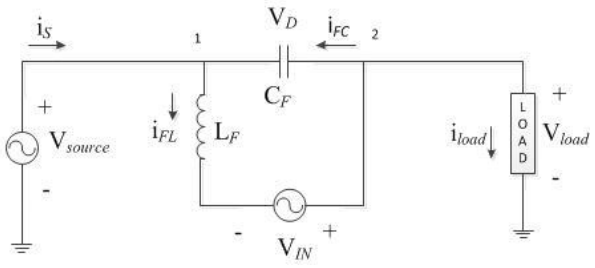

Figure 2. Dynamic voltage restorer schematic circuit.

Parameters of filter L_F and C_F in Figure 2 are used to tune the AC output of IGBT based VSC. Filter inductor current and filter capacitor current are described by i_{FL} and i_{FC} respectively.

$$i_{FC} = C_F \frac{dV_D}{dt} \tag{2}$$

By applying Kirchhoff's current law at node 1 in Figure 2 we get the following equation.

$$i_S + i_{FC} + i_{FL} = 0 \tag{3}$$

Now we will put value of i_{FC} from equation (2) in equation (3).

$$i_S + C_F \frac{dV_D}{dt} - i_{FL} = 0 \tag{4}$$

$$C_F \frac{dV_D}{dt} = i_{FL} - i_S \tag{5}$$

$$\frac{dV_D}{dt} = \frac{1}{C_F}(i_{FL} - i_S) \tag{6}$$

Equation (6) is the 1st state equation. Now we apply Kirchhoff's voltage law at the closed loop in Figure 2 to get 2nd state equation.

$$L_F \frac{di_{FL}}{dt} - V_{IN} + V_D = 0 \tag{7}$$

$$L_F \frac{di_{FL}}{dt} = V_{IN} - V_D \tag{8}$$

$$\frac{di_{FL}}{dt} = \frac{1}{L_F}(V_{IN} - V_D) \tag{9}$$

Thus the state space model of DVR is described by equations (6) and (9).

$$\frac{d}{dt}\begin{bmatrix} i_{FL} \\ V_D \end{bmatrix} = \begin{bmatrix} 0 & -1/L_F \\ 1/C_F & 0 \end{bmatrix}\begin{bmatrix} i_{FL} \\ V_D \end{bmatrix} + \begin{bmatrix} 0 & 1/L_F \\ -1/C_F & 0 \end{bmatrix}\begin{bmatrix} i_S \\ V_{IN} \end{bmatrix} \tag{10}$$

i_{FL} and V_D are the state variables, while i_S and V_{IN} are the input variables. A sliding manifold is selected that will control the output of inverter. As first derivative of V_D do not have control input V_{IN}, therefore second derivate will be calculated.

$$\text{Let} \quad \frac{dV_D}{dt} = \frac{1}{C_F}(i_{FL} - i_S) = x_1 \tag{11}$$

$$\frac{dx_1}{dt} = \frac{1}{C_F}\left(\frac{di_{FL}}{dt} - \frac{di_S}{dt}\right) \tag{12}$$

Putting value $\frac{d\,i_{FL}}{dt}$ from equation (9) in equation (12) we get

$$\frac{dx_1}{dt} = \frac{1}{C_F}\left(\frac{1}{L_F}(V_{IN} - V_D) - \frac{di_S}{dt}\right) \tag{13}$$

$$\frac{d}{dt}\begin{bmatrix} V_D \\ x_1 \end{bmatrix} = \begin{bmatrix} x_1 \\ \frac{1}{C_F}.\frac{1}{L_F}V_{IN} - \frac{1}{C_F}.\frac{1}{L_F}V_D) - \frac{1}{C_F}.\frac{di_S}{dt} \end{bmatrix} \tag{14}$$

Therefore, the difference of reference voltage and voltage injected by DVR is the selected criteria for proposed strategy for sliding manifold as it can control output of DVR.

$$S = (V_{DREF} - V_D) + k\left(\frac{dV_{DREF}}{dt} - \frac{dV_D}{dt}\right) \tag{15}$$

To insure existence of operation and bring state variables to sliding manifold the following two conditions must be satisfied

$$S = 0, \quad \dot{S} = 0$$

The switching law can be devised as

$$U = \begin{cases} +1 \ \textit{if} \ S > +\varepsilon \\ -1 \ \textit{if} \ S < -\varepsilon \end{cases} \tag{16}$$

Value of switching control variable (U) is chosen based on a constant ε.

To reduce chattering phenomena introduced in standard sliding modes, super twisting control is utilized to generate control signals for VSC. The control law is given in equation 17 [22-24].

$$\gamma = -\lambda_1 \left| S \right|^{1/2} \operatorname{sgn}(S) - \lambda_2 \int \operatorname{sgn}(S)\, ds \tag{17}$$

The control law given in equation 17 has two constants λ_1 and λ_2 . These constants are tuning quantities for unwanted switching of components. Signum of sliding manifold, sgn(S), gives +1 output if S is greater than zero and -1 if S is less than zero. Based on this control law gating signals are generated for VSC. The desired voltage magnitude is produced by VSC and injected at PCC using injection transformer.

3. Design Specifications

The control technique used will mitigate voltage sag and voltage swell while considering following three conditions.

1. The equipment sensitivity curve devised by ITIC and SEMI F-47 shows that equipments can tolerate outage upto one cycle. Thus the control strategy must ensure to detect and mitigate voltage sag and voltage swell within one cycle (20 milli seconds) at power frequency.
2. Usually electrical loads are designed to tolerate voltage variation upto $\pm$ 10%. While the proposed technique takes no correcting action if voltage at any time is lower by 5% of rated load voltage.
3. The difference of utility voltage and the rated load voltage is called as error voltage. This error voltage must only be injected or absorbed by the control strategy.

4. Super-Twisting Sliding Mode Control of DVR

Control strategy proposed in this research detects and corrects the voltage sag and voltage swell within 2 milli seconds. Instead of using standard sliding mode control, chattering is reduced by using super-twisting controller for the system of relative degree of 1. The block diagram of super-twisting SMC for dynamic voltage restorer is given in Figure 3. The reference signal generation block subtracts the reference voltage and actual utility voltage. The resultant voltage is then subtracted from actual injected voltage.

4.1 Selection of Sliding Surface

Sliding manifold described by signal S in Figure 4 is based on the calculated error voltage V_{DREF}. This sliding surface is designed based on equation 15 given in Section 2 of the paper. V_D is the feedback signal of closed loop super-twisting sliding mode control. Difference of V_D and V_{DREF} and their derivatives compose the sliding surface.

A comparator is then applied on S with ε as reference quantity. The generated value is passed through a multiplexer to apply switching law on a single signal. Super-Twisting control law is applied on the sliding surface.

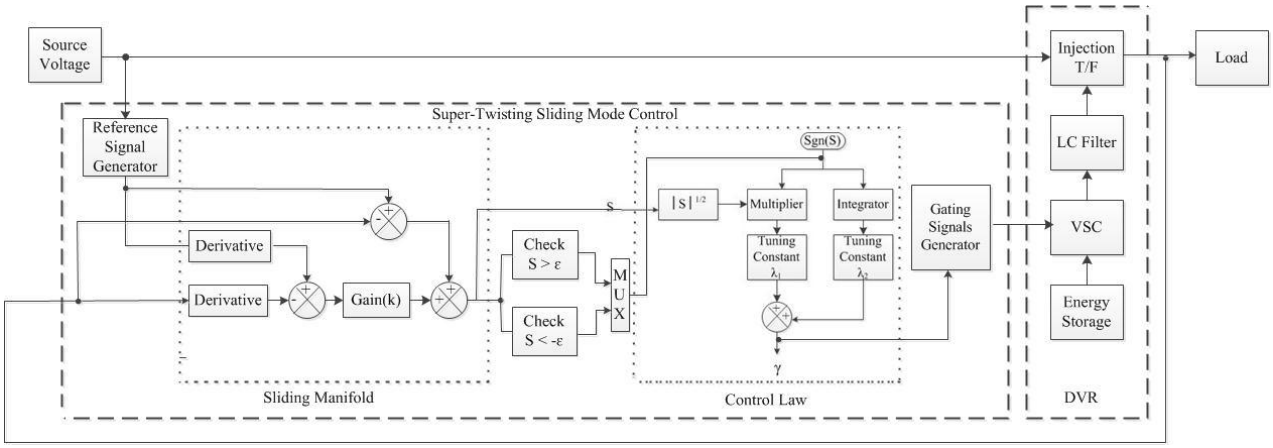

Figure 3. Block Diagram of closed loop feed back control of DVR.

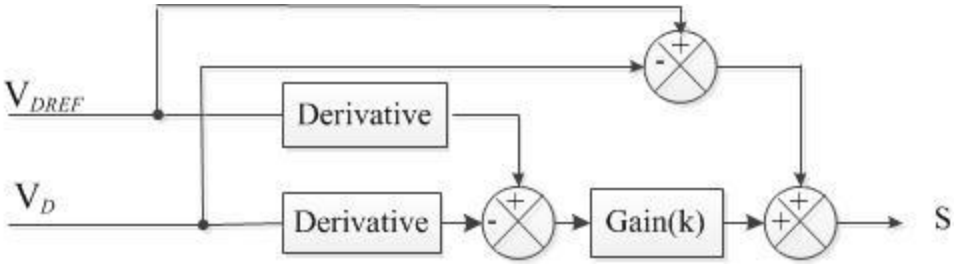

Figure 4. Block Diagram of sliding manifold.

4.2 Control Law

Control law has basically two parts as described in Section 2. In first part multiplier output is tuned by a parameter λ_1. Modulus of sliding manifold and multiplexer output are used as inputs to multiplier. In second part of control law an integral block is used to filter out high frequency components. The output is further modified by parameter λ_2. The term containing modulus and signum of sliding manifold reduce switching of components, thereby increasing life of components. While the integral term corresponds to low pass filter. The overall result is fast response, less chattering and robustness to external parameters changes. Block diagram of super-twisting SMC switching law is given in Figure 5.

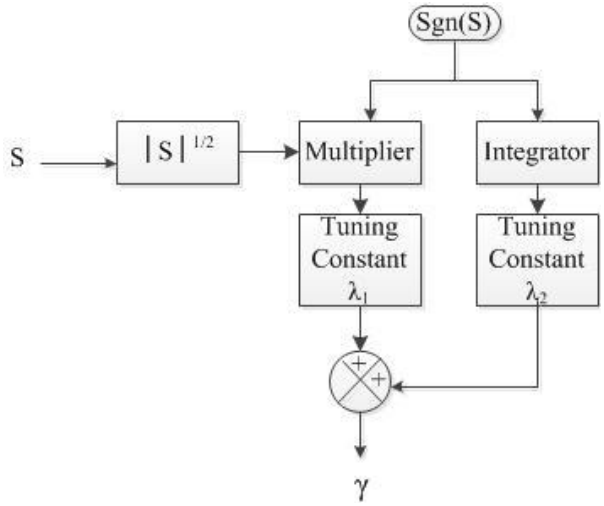

Figure 5. Switching law of super-twisting SMC.

4.3 Generation of Injected Voltage

A demultiplexer is used to generate four signals for VSC. Thus the output of control is used to switch semiconductor IGBT switches of VSC. A 24V dc battery source is used as DC energy storage device. VSC converts DC to AC upon application of gating signals during voltage sag and voltage swell. The AC output of converter is passed through a low pass LC filter. The designed filter has an inductance of 1.8 mH and a

Table 1. Test system parameters.

Component/Parameter Description	Value	Units
Utility voltage	240	V
System apparent power	1000	VA
DC source voltage	24	V DC
System frequency	50	Hz
Voltage sag/swell detection and mitigation time	<2	ms
Injection transformer power rating	1000	VA
Injection transformer voltage ratio	24/240	-
Filter inductor	1.8	mH
Filter capacitor	5.5	mF
Control action	Super-Twisting Sliding Mode	

capacitance of 5.5 mF. The filtered output is injected through injection transformer. The injection transformer of 1:10 voltage ratio is selected for desired results.

5. Simulation Results

The effectiveness of super-twisting control strategy for DVR is examined by developing a test system in SimPowerSystems™ environment. The simulations are carried out for single phase system with voltage sag and voltage swell of different magnitude in MATLAB®/SIMULINK®. Per phase voltage of three phase power system voltage source is 240V. DVR is used to maintain 240V per phase voltage across the load. DVR setup consist of DC battery source, Pulse Width Modulation based voltage source converter, LC low pass filter and 1:10 ratio injection transformer. The power consumption of load for each phase is 816VA. Thus for 240V the rated current is 3.4A. Injection transformer's voltage ratio is 24:240. Primary winding (24V) is connected with voltage source converter. Secondary winding (240V) is connected with distribution network. From MATLAB® simulations results values of utility, DVR and load voltages are measured. Active and reactive power of load is also tested during voltage sag, voltage swell and phase jump. The simulation plots are given in Figure 6 to Figure 21. The test system is based on the following parameters (Table 1).

Proposed super-twisting sliding mode control strategy is applied on following PQ problems.

(a) Voltage sags of different depths in utility supply.

(b) Voltage swells of different magnitude in utility supply.

(c) Phase jumps in utility supply.

5.1 Compensation of Voltage Sag

Result of 30% sag depth that starts at 0.04 sec and lasts until 0.1 sec is shown in Figure 6. The designed controller compensates for the disturbance. The graph shows that load and utility voltage completely overlap other than this sag duration. Utility, load and DVR injected voltages are shown with red (straight), blue (dashed) and black (doted) colors respectively. The plots in Figure 6 indicates that during normal operation, no voltage is injected by DVR. Whereas when voltage sag occurs the control scheme detects it and injects a voltage for sag compensation within 2 milli sec. as compared to 20 milli sec. standard time of compensation. From this graph it is also evident that DVR only injects the missing voltage level. For a peak value of utility supply of 339.4V under normal conditions, 30% sag will result in voltage drop upto 237.6V. Then the magnitude of DVR injected voltage is 101.8V. Figure 7 shows the error signal while Figure 8 shows inverter output voltage during 30% sag in utility voltage. From Figures 6, 7 and 8 it is evident that injected voltage by DVR becomes zero after sag termination. Inverter output voltage is filtered out to remove high frequency components. Voltage THD for the

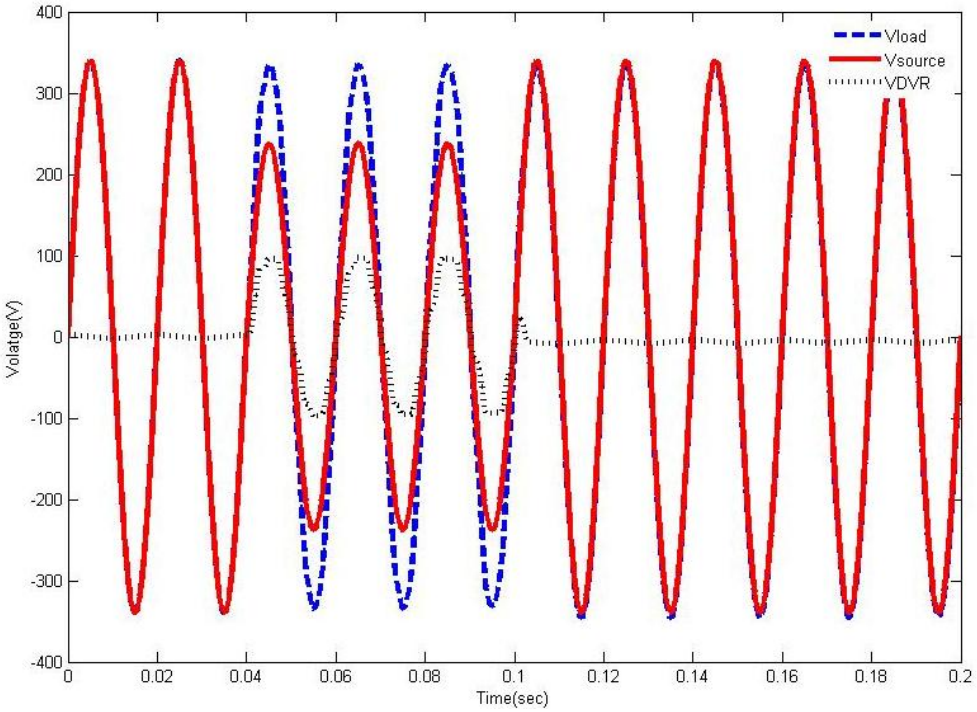

Figure 6. Load voltage compensation for 30% sag.

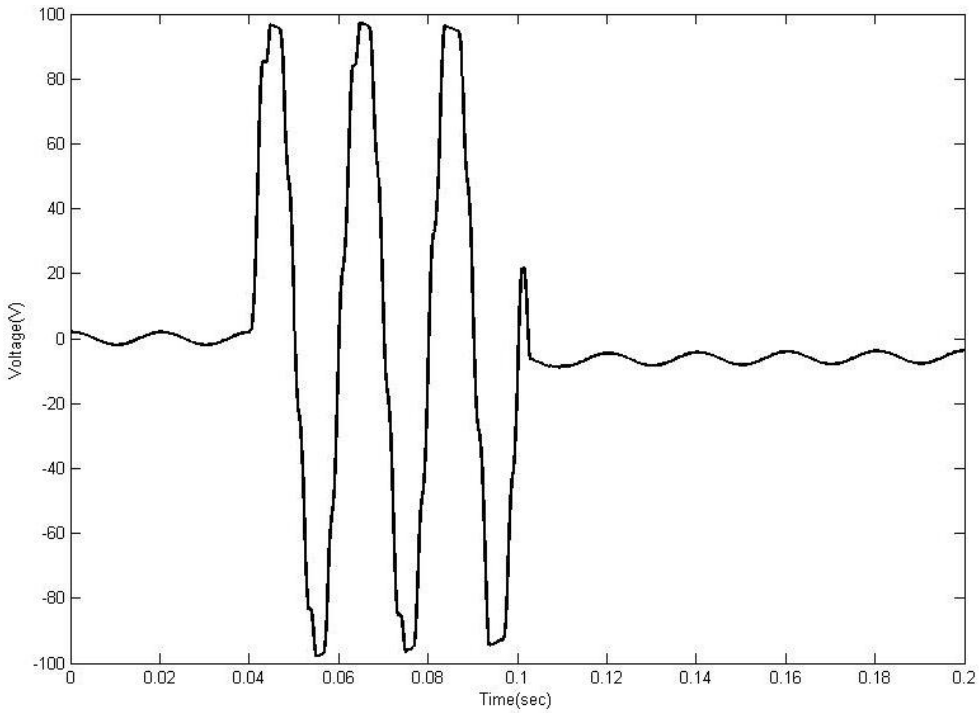

Figure 7. DVR injected voltage for 30% sag.

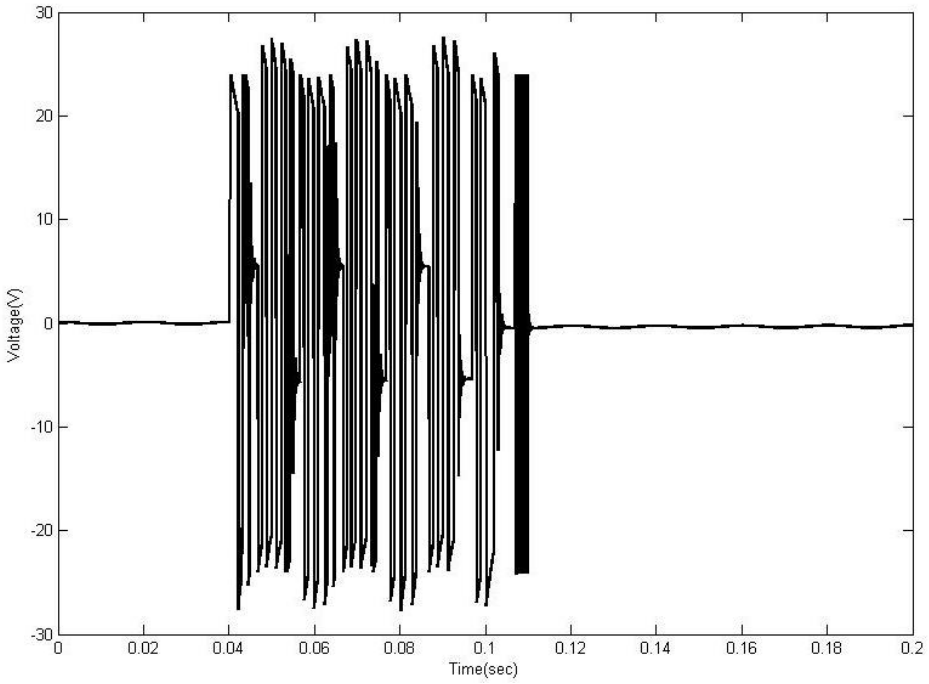

Figure 8. VSC output voltage for 30% sag.

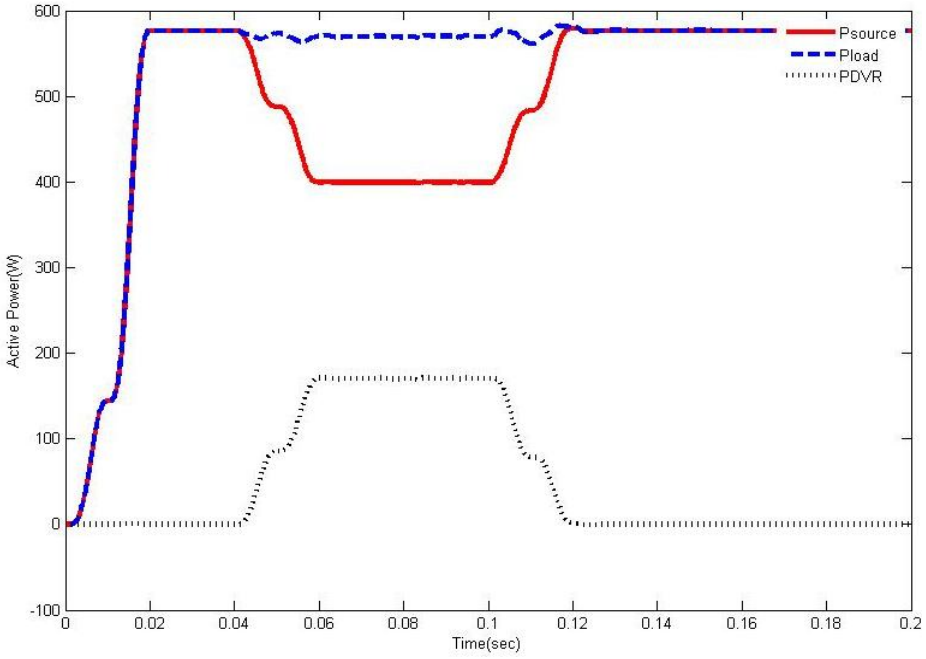

Figure 9. Real Power during 30% sag.

proposed control scheme is 0.45%. Thus harmonic content of load voltage is reasonably less than 5% which is suggested by IEEE Std. 1159-1995. Figures 9 and 10 show real and reactive power plots respectively. DVR control scheme also smoothes the real and reactive power drawn by load during compensation mode. Simulation results show that the active power from utility decreases from 580W to 400W during 30% voltage sag. DVR generates about 180W active power during voltage sag event to regulate power flow to load.

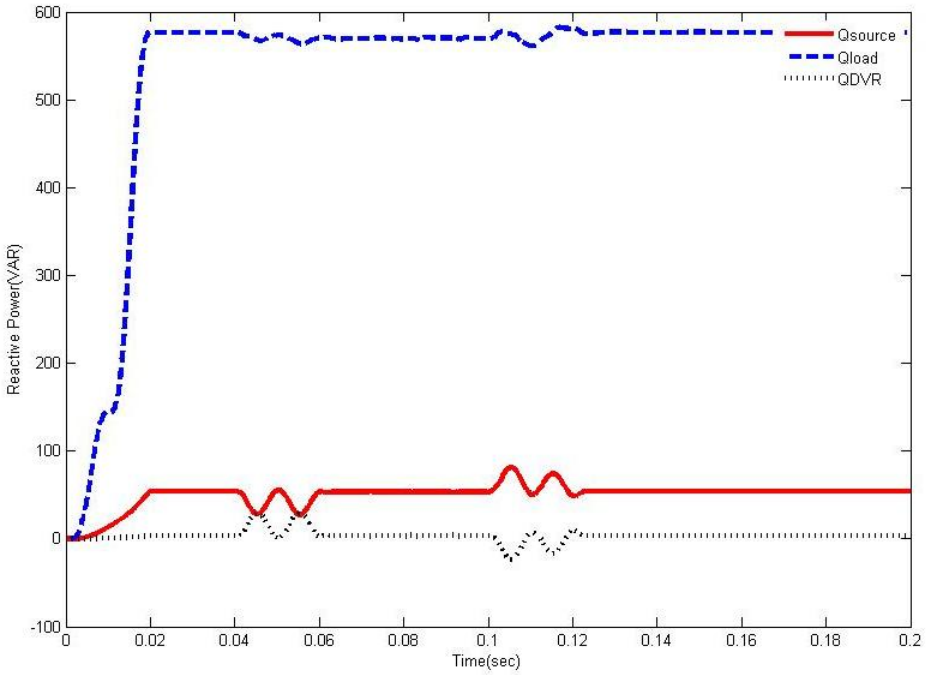

Figure 10. Reactive Power during 30% sag.

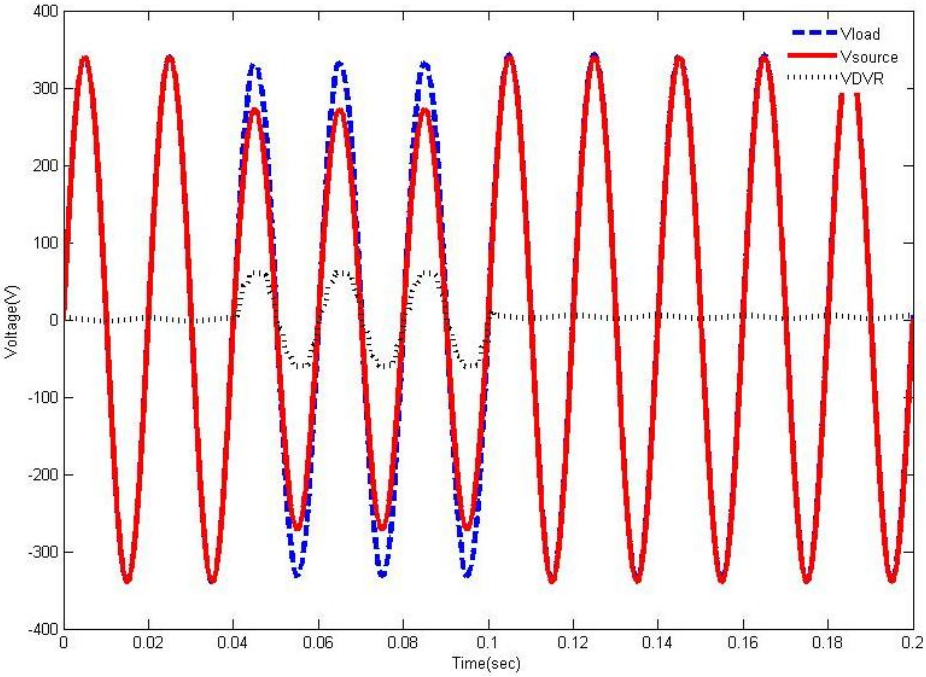

Figure 11. Load voltage compensation for 20% sag.

Voltage sag of different magnitudes is chosen to check the performance of proposed control scheme of DVR. Control of DVR has efficiently handled the voltage sag of depth of 20% and 40% as described by Figures 11 and 12 respectively.

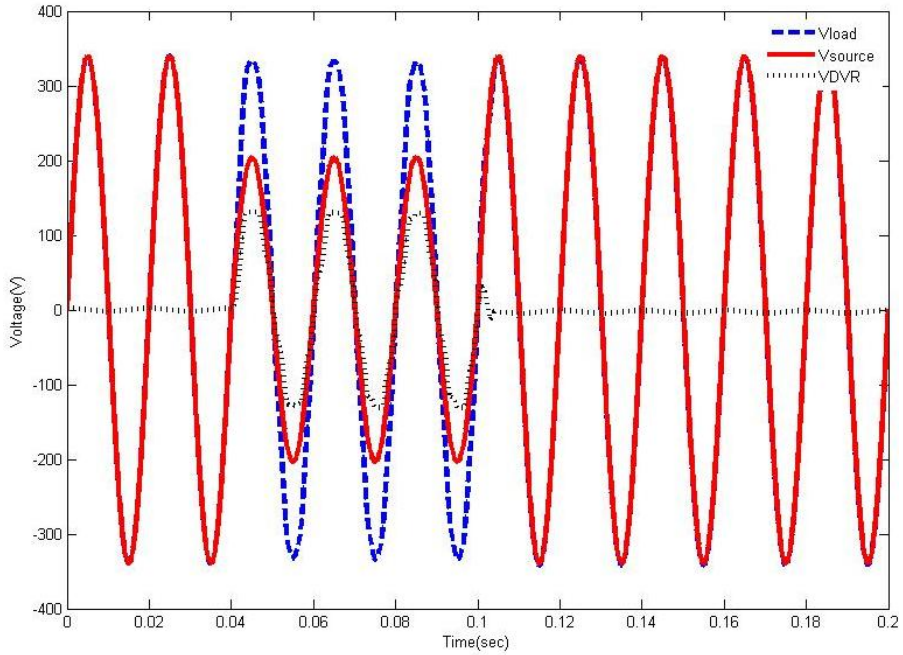

Figure 12. Load voltage compensation for 40% sag.

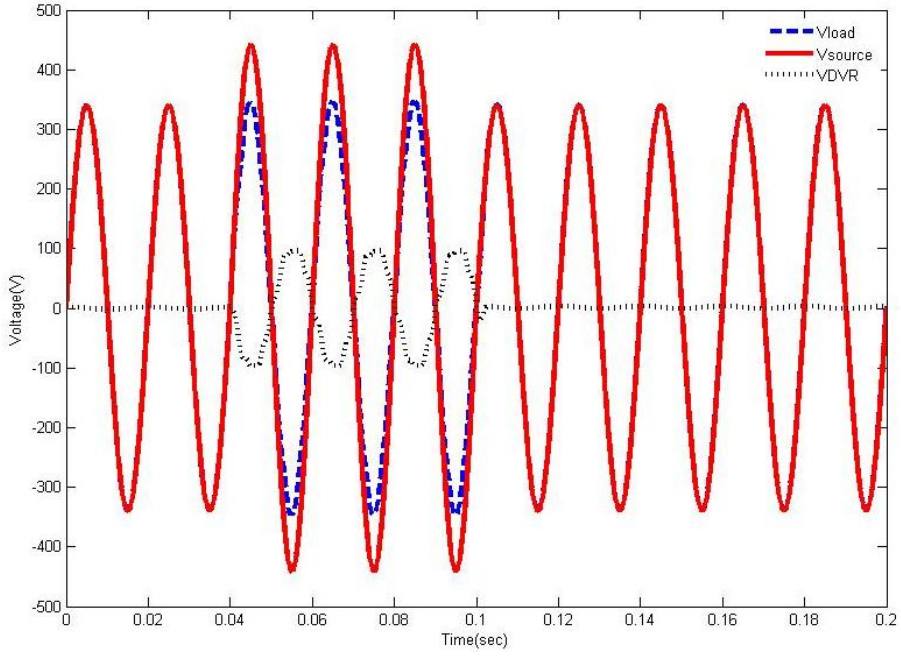

Figure 13. Load voltage compensation for 30% swell.

5.2. Compensation of Voltage Swell

Voltage swell occurs at 0.04 sec and lasts until 0.1 sec with amplitude of 30%. The simulated results for the voltage swell are plotted in Figure 13 to Figure 17. The simulations indicate that the fast response of super-twisting sliding mode maintains load voltage profile of sensitive loads to ITIC standard. The distortion in supply voltage due to voltage swell is corrected within 2 milli sec. Figure 14 shows the compensated DVR voltage for voltage swell. The calculated voltage THD is 0.45%. The THD value is within standard limit. The inverter output voltage is shown in Figure 15. The

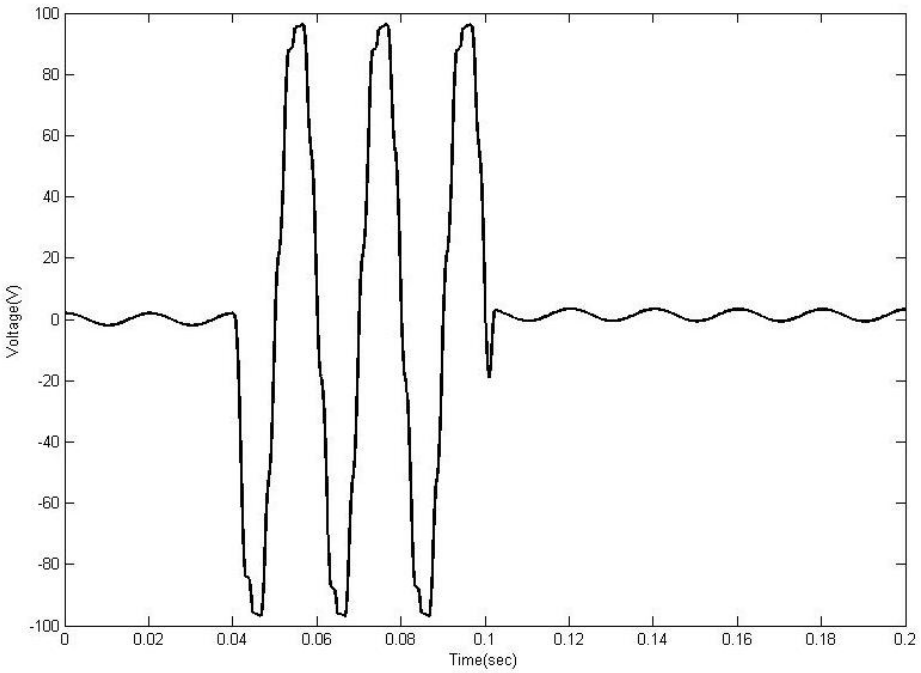

Figure 14. DVR injected voltage for 30% swell.

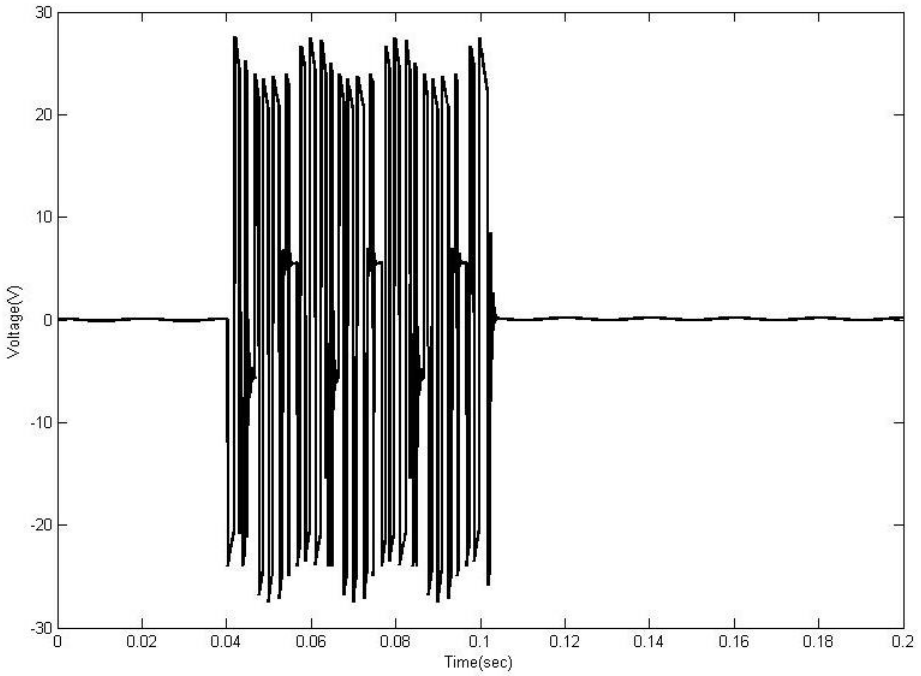

Figure 15. Voltage Source Converter output voltage for 30% swell.

real and reactive power of utility, load and DVR is shown in Figure 16 and Figure 17 respectively. DVR also compensates real and reactive power of load. Increase in active power of utility from 580W to 770W is seen during 30% voltage swell in utility voltage. Compensation is done by DVR with absorption of 190W power. The proposed control is also tested to check the performance for 20% and 40% increase of utility voltage. Figure 18 and Figure 19 show the results, thereby validating the super-twisting sliding mode control of DVR.

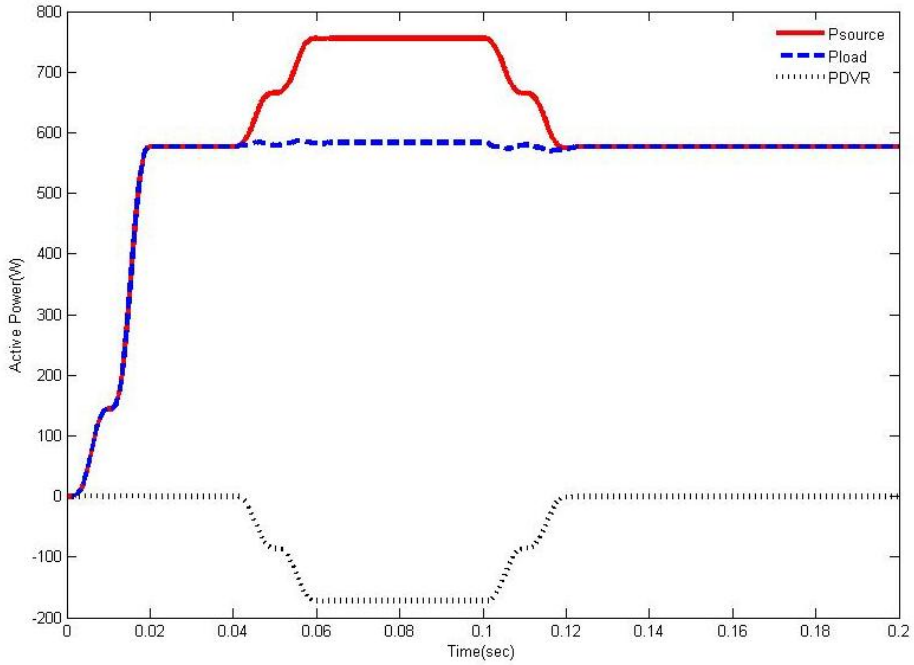

Figure 16. Real power for 30% swell

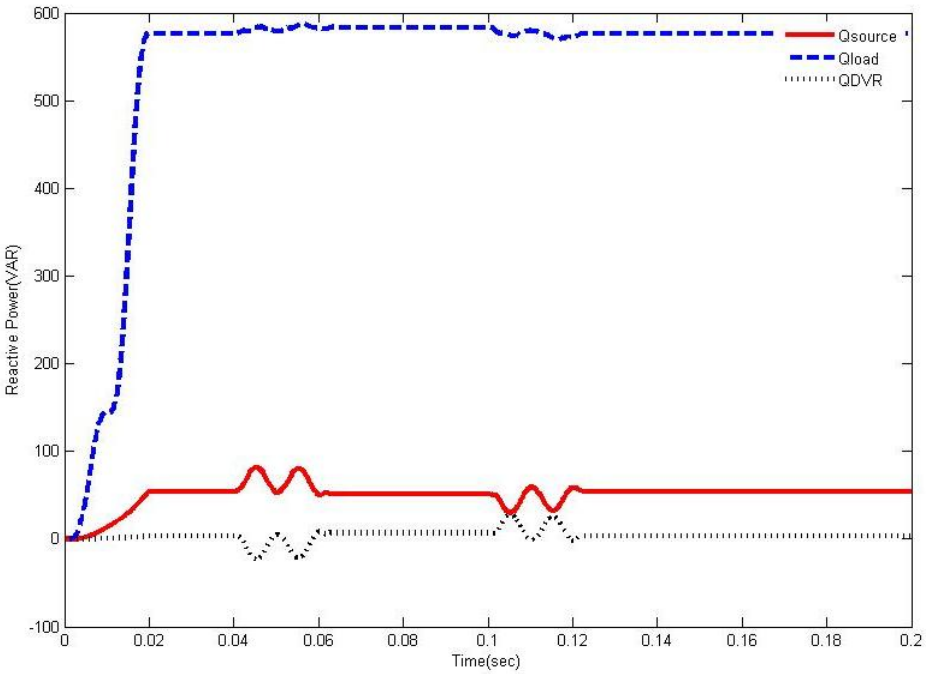

Figure 17. Reactive power for 30% swell.

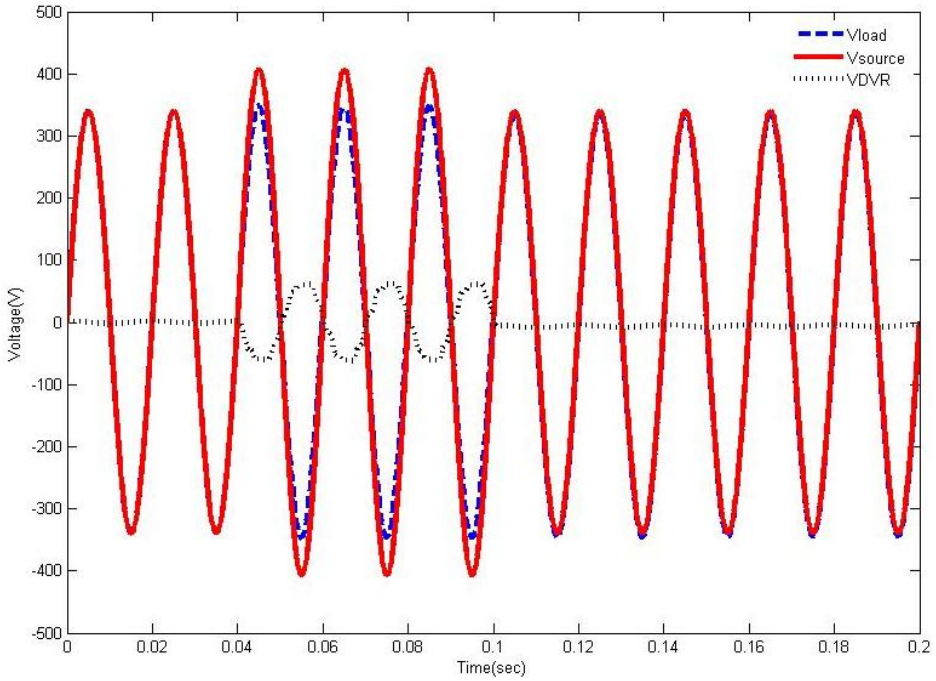

Figure 18. Load voltage compensation for 20% swell.

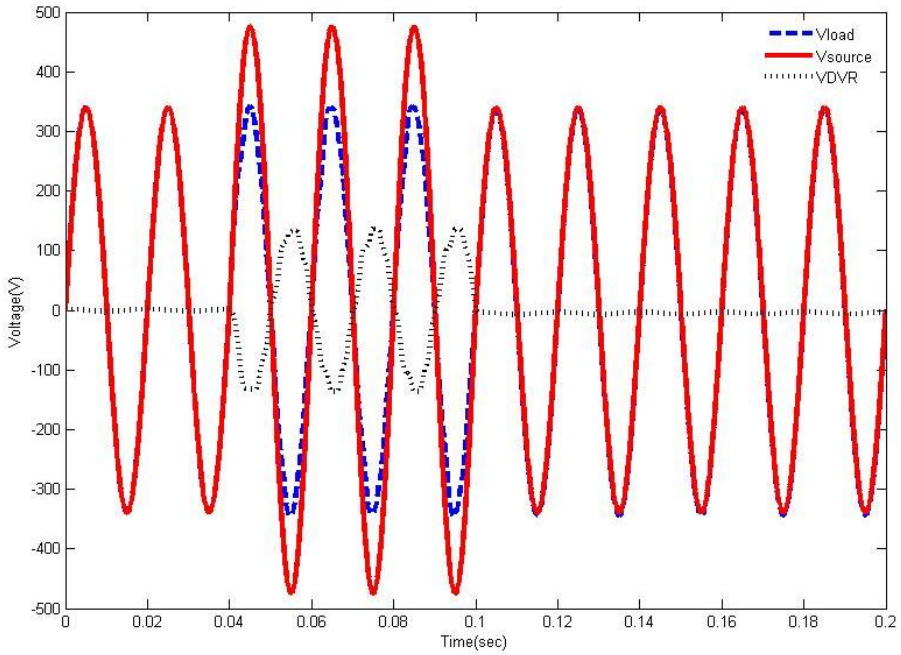

Figure 19. Load voltage compensation for 40% swell

5.3 Compensation of Phase Jumps

Loads sensitive to phase jumps can be compensated using proposed technique. The simulation results in Figure 20 gives the dynamic voltages of utility, load and DVR for 20 degree phase jump. The simulation shows behavior of proposed control strategy when there is no voltage sag but only a phase jump. DVR injects a voltage to compensate phase-shift occurred in utility voltage. Voltage injected from DVR becomes zero

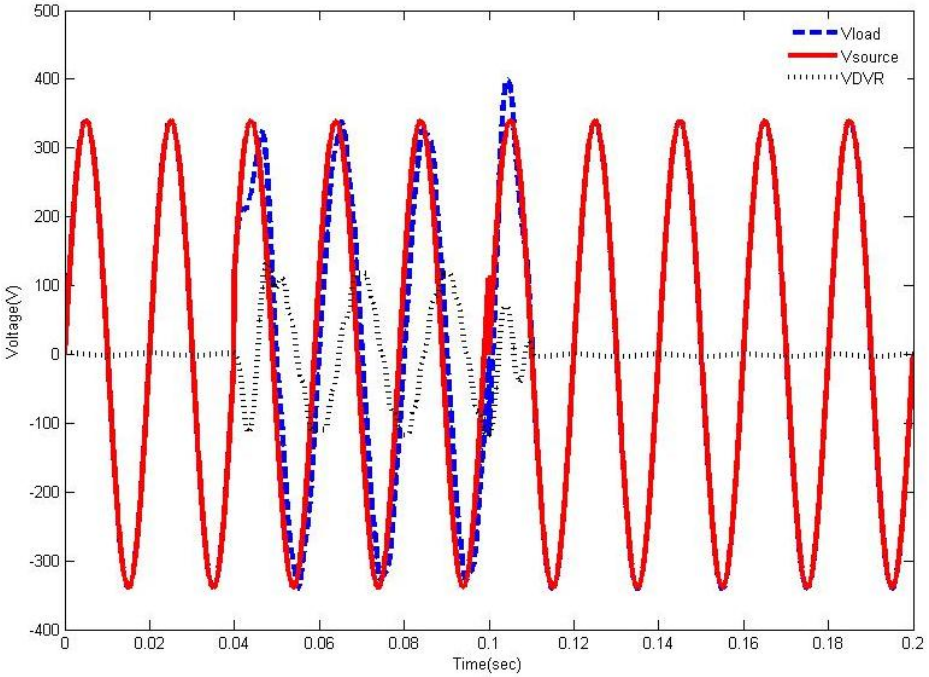

Figure 20. Load voltage compensation for +20° phase jump.

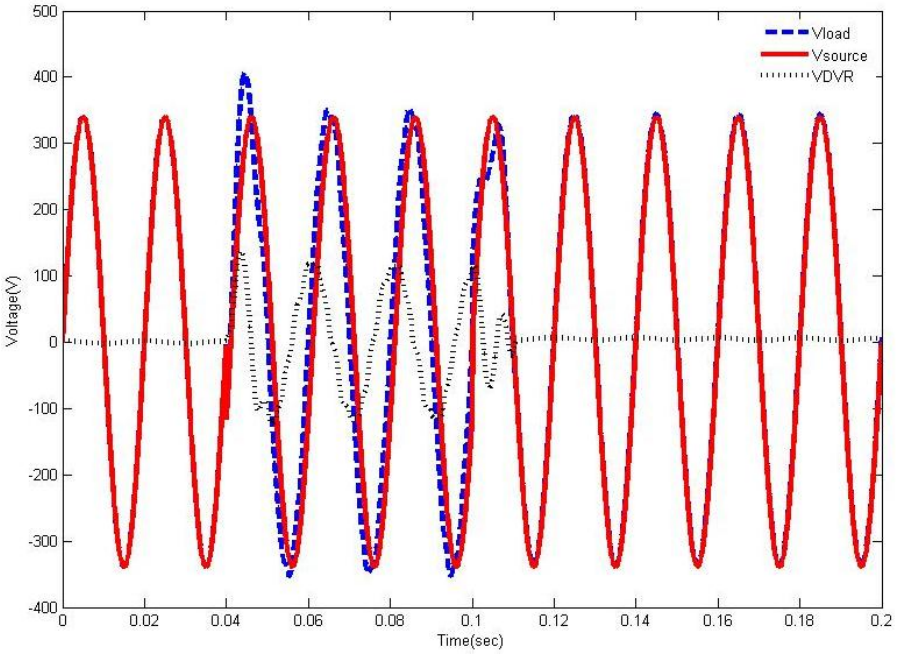

Figure 21. Load voltage compensation for -20° phase jump.

after termination of phase jump event. Figure 20 shows that in load voltage a spike (transient disturbance) occurred at termination of phase jump which is undesirable but as it lasts for only 2 milli sec. thereby load voltage waveform is not affected considerably. Thus overall effect of utility voltage phase jump is neutralized by proposed control strategy of DVR.

In Figures 20 and 21 phase jump is considered and voltage profile of utility, load and DVR shows

that phase jumps can be catered using proposed control strategy. DVR injects a voltage to compensate phase-shift occurred in utility voltage. Voltage injected from DVR becomes zero after termination of phase jump event. Figure 21 shows that in load voltage a spike (transient disturbance) occurred at start of phase jump which is undesirable but as it lasts for only 2 milli sec. thereby load voltage waveform is not affected considerably. This happens when DVR operation starts for compensation of phase jump. Thus overall effect of utility voltage phase jump is neutralized by proposed control strategy of DVR.

6. Conclusion

This paper has presented a new method for compensation of voltage sag, voltage swell and phase jump in power distribution network. Control system of DVR is based on second order super-twisting SMC. The method provides finite-time convergence, robustness to disturbances and minimum chattering. Simulation results validate the system. The presented control scheme can compensate voltage sags, voltage swells and phase jumps within 2ms which is reasonably lower than ITIC curve and SEMI-F-47 standard for sensitive loads that suggest a tolerable time limit of 20ms.

Acknowledgement

The authors gratefully acknowledge the technical discussion with Dr. Qudrat Khan.

References

[1] M. H. J. Bollen, Understanding Power Quality Problems: Voltage Sags and Interruptions, New York, IEEE Press (2000).

[2] C. Olarte, J. Gonzalez and J. Perez, Study and Analysis of Voltage Dips in an Adjustable Speed Drives, Proceedings of 11th International Conference on Renewable Energies and Power Quality, Spain (April 2010) pp. 319-323.

[3] R.C. Dugan, M.F. McGranaghan, S. Santoso and H.W. Beaty, Electrical Power Systems Quality, McGraw-Hill (2004).

[4] J. Wang, S. Chen and T. T. Lie, Estimating Economic Impact of Voltage Sags, Proceedings of IEEE International Conference on Power System Technology, Singapore (2004) pp. 350-355.

[5] J. Wang, S. Chen and T. T. Lie, IEEE Transactions on Power Delivery **20**, No. 2 (2005) 1738.

[6] P. T. Nguyen and T. K. Saha, Dynamic Voltage Restorer Against Balanced and Unbalanced Faults: Modeling and Simulations, IEEE-School of Information Technology and Electrical Engineering, University of Queensland, Australia (2004) pp. 1-6.

[7] N.H. Woodley, L. Morgan and A. Sundaram, IEEE Transactions on Power Delivery **14**, No. 3 (1999) 1181.

[8] A. Ghosh and G. Ledwich, Power Quality Enhancement using Custom Power Devices, Kluwer Academic Publishers (2002).

[9] S.M. Silva, F. A. Eleuterio, A. D. S. Reis and B.J.C. Filho, Protection Schemes for a Dynamic Voltage Restorer, Proceedings of IEEE Industry Application Conference, Seattle, Washington, USA (2004) pp. 2239-2243.

[10] A. Pakharia and M. Gupta, International Journal of Advances in Engineering & Technology **4**, No. 1 (2012) 347

[11] R.H. Salimin and M.S.A. Rahim, Simulation Analysis of DVR Performance for Voltage Sag Mitigation, Preceedings of 5th International Power Engineering and Optimization Conference (PEOCO2011), Malaysia (6-7 June 2011) p. 261.

[12] B. Ferdi, C. Benachaiba, S. Dib and R. Dehini, Journal of Electrical Engineering, Theory and Application **1**, No.3 (2010) 165.

[13] D.D. Chowdary and G.V. Nagesh Kumar, Indian Journal of Science and Technology **1**, No. 5 (2008) 1.

[14] M.V. Jithesh and P.A. Michael, International Journal of Engineering and Advanced Technology **2**, No. 2 (2012) 281.

[15] A. Ishigame, T. Furukawa, S. Kawamoto and T. Taniguchi, IEEE Trans. on Industrial Electronics **40**, No. 1 (1993) 64.

[16] S. Chen, G. Joos, L. Lopes and W. Guo, A Nonlinear Control Method of Dynamic Voltage Restorers, Proc. IEEE 33rd Annual Power Electronics Specialists Conference (2002) pp. 88- 93.

[17] M.I. Marei, E.F. El-Saadany and M.M.A. Salama, IEEE Transactions on Power Delivery **22**, No. 4 (2007) p. 2017.

[18] H. Kim and S.K. Sul, IEEE Transactions on Power Electronics **20**, No. 5 (2005) p. 1169.

[19] Vilathgamuwa, Perera, Choi, IEEE Transactions on Power Delivery **18**, No. 3 (2003) 928.

[20] A. Levant, International Journal of Control, Taylor & Francis Ltd. **76**, No. 9/10 (2002) 924.

[21] H. Kizmaz, S. Aksoy and A. Muhurcu, Sliding Mode Control of Suspended Pendulum, Proceedings of the International Symposium on Modern Electric Power Systems (MEPS), Wroclaw (Sept. 2010) pp. 20-22.

[22] A. Levant, International Journal of Control, Taylor & Francis Ltd. **58**, No. 6 (1993) 1247.

[23] W.B. Lin, H.K. Chiang, Artificial Life and Robotics **16**, No. 3 (2011) 307.

[24] S.V. Emel'yanov, S.K. Korovin and A. Levant, Computational Mathematics and Modeling **7**, No. 3 (1996) 294.